Interdigitated Deletion Complexes on Mouse Chromosome 5 Induced by Irradiation of Embryonic Stem Cells

John C. Schimenti,[1,5] Brian J. Libby,[1] Rebecca A. Bergstrom,[1] Lawriston A. Wilson,[1] Dieter Naf,[1] Lisa M. Tarantino,[2,3] Alireza Alavizadeh,[2] Andreas Lengeling,[2,4] and Maja Bucan[2]

[1]The Jackson Laboratory, Bar Harbor, Maine 04609 USA; [2]University of Pennsylvania School of Medicine, Philadelphia, Pennsylvania 19104-6140 USA; [3]Genomics Institute of the Novartis Research Foundation, San Diego, California 92121 USA

Chromosome deletions have several applications in the genetic analysis of complex organisms. They can be used as reagents in region-directed mutagenesis, for mapping of simple or complex traits, or to identify biological consequences of segmental haploidy, the latter being relevant to human contiguous gene syndromes and imprinting. We have generated three deletion complexes in ES (Embryonic Stem) cells that collectively span ~40 cM of proximal mouse chromosome 5. The deletion complexes were produced by irradiation of F_1 hybrid ES cells containing herpes simplex virus thymidine kinase genes (*tk*) integrated at the *Dpp6*, *Hdh* (Huntington disease locus), or *Gabrb1* loci, followed by selection for *tk*-deficient clones. Deletions centered at the adjacent *Hdh* and *Dpp6* loci ranged up to ~20 cM or more in length and overlapped in an interdigitated fashion. However, the interval between *Hdh* and *Gabrb1* appeared to contain a locus haploinsufficient for ES cell viability, thereby preventing deletions of either complex from overlapping. In some cases, the deletions resolved the order of markers that were previously genetically inseparable. A subset of the ES cell–bearing deletions was injected into blastocysts to generate germline chimeras and establish lines of mice segregating the deletion chromosomes. At least 11 of the 26 lines injected were capable of producing germline chimeras. In general, those that failed to undergo germline transmission bore deletions larger than the germline-competent clones, suggesting that certain regions of chromosome 5 contain haploinsufficient developmental genes, and/or that overall embryonic viability is cumulatively decreased as more genes are rendered hemizygous. Mice bearing deletions presumably spanning the semidominant hammertoe locus (*Hm*) had no phenotype, suggesting that the classic allele is a dominant, gain-of-function mutation. Overlapping deletion complexes generated in the fashion described in this report will be useful as multipurpose genetic tools and in systematic functional mapping of the mouse genome.

The Human Genome Project is transitioning into the so-called "Post-Genomics" era, in which the emphasis in genome research is switching from structure to function. This change is spawning new technologies and concepts for conducting functional analyses on a comprehensive, large scale, including gene expression chips, protein interaction assays, and computational tools to infer function from DNA sequence. However, a true understanding of the role of a gene in the context of a whole organism depends on analysis of mutations or allelic variation. Presently, the infrastructure and technology for understanding the molecular genetic basis of phenotypically defined mammalian genes has outstripped the supply of human disease alleles and mouse mutants.

As with the two general strategies being used for genomic sequencing —whole genome shotgun versus a systematic sequencing of chromosome regions (Green 1997; Weber and Myers 1997)—there are two general approaches for mutagenesis: whole genome versus region directed. The former approach involves three generation screens for recessive mutations located throughout the genome. The latter typically involves the use of deletions to saturate particular chromosome regions for randomly induced point mutations. The relative merits of each approach have been discussed in detail elsewhere (Schimenti and Bucan 1998) but can be summarized as follows. Genome-wide scans have the advantage of yielding more mutants, but their map locations are unknown. Region-specific mutagenesis has the advantage of restricting the location of new mutations to a known region, thereby facilitating genetic mapping. It is also advantageous for the identification and propagation of steriles and lethals. However, this approach requires the availability of special chromosomes (inversions/deletions), and the mutations identified are limited to a small fraction of the genome. Ready availability of deletion stocks

[4]Present address: Institute of Mammalian Genetics, GSF-National Research Center for Environment and Health, 85764 Neuherberg, Germany.
[5]Corresponding author.
E-MAIL jcs@jax.org; FAX (207) 288-6082.

would alleviate this drawback and open new avenues for directed functional analyses of particular chromosomal regions.

Here, we report the generation of three deletion complexes—collections of nested deletions—spanning ~ 40 cM of mouse chromosome 5. These deletions were induced by irradiation of ES cell clones containing targeted insertions of a negatively selectable (*tk*) reporter. Deletions centered around two of the three DFPs (Deletion Focal Points) overlap in an interdigitated manner, allowing one to systematically characterize functional regions of this chromosome by pairwise combination of the deletions through mating. These deletions also will serve as reagents in a region-directed ENU (Ethylnitrosourea) saturation mutagenesis screen and in the modeling of the Wolf-Hirschhorn contiguous gene syndrome that resides in this region.

RESULTS

Targeted Insertions of a TK-neo Cassette at the Hdh, Dpp6, and Gabrb1 Loci

To create a series of deletions spanning the proximal region of mouse chromosome 5, the technique of irradiating F_1 hybrid ES cells was used (You et al. 1997a, 1997b; Thomas et al. 1998). This strategy entails the targeted insertion of a *tk*-expressing cassette into a locus of choice, treatment of targeted cells with radiation, and selection for loss of *tk* expression with the drug FIAU (1–2′-deoxy-2′-fluoro-β-D-arabinofuranosyl-5-iodouracil). The loci chosen for targeting the *tk* cassette, *Dpp6*, *Hdh*, and *Gabrb1,* are distributed across the region spanned by the rump white (*Rw*) inversion. The proximal breakpoint of this inversion lies within *Dpp6*, and the distal end lies near the *Kit* (formerly *W*) locus (Fig. 2; Hough et al. 1998). This inversion serves as a balancer that is important for downstream saturation mutagenesis screens (Schimenti and Bucan 1998; see Discussion).

The *Hdh* locus of v6.4 F_1 hybrid ES cells (C57BL/6J × 129/Jae) (You et al. 1998) was targeted (Fig. 1a) with a *tk*-neomycin resistance (neo) cassette (You et al. 1997a) by modifying a vector previously used to generate a null mutation in this gene (Duyao et al. 1995; Fig. 1a) Eighty-seven of 261 (33.3%) G418-resistant clones examined contained a targeted integration. Vectors (Fig. 1b,c) for the *Dpp6* and *Gabrb1* loci also resulted in successful targeting by homologous recombination in the v6.4 line, at overall frequencies of 6/347 (1.7%) and 24/93 (26%), respectively.

Before induction of deletions, it is important to select targeted clones that retain germline-colonizing potential. Accordingly, several clones from each targeted locus were first karyotyped, and two or three of those with a euploid chromosome mode were injected into blastocysts to check for germline transmission.

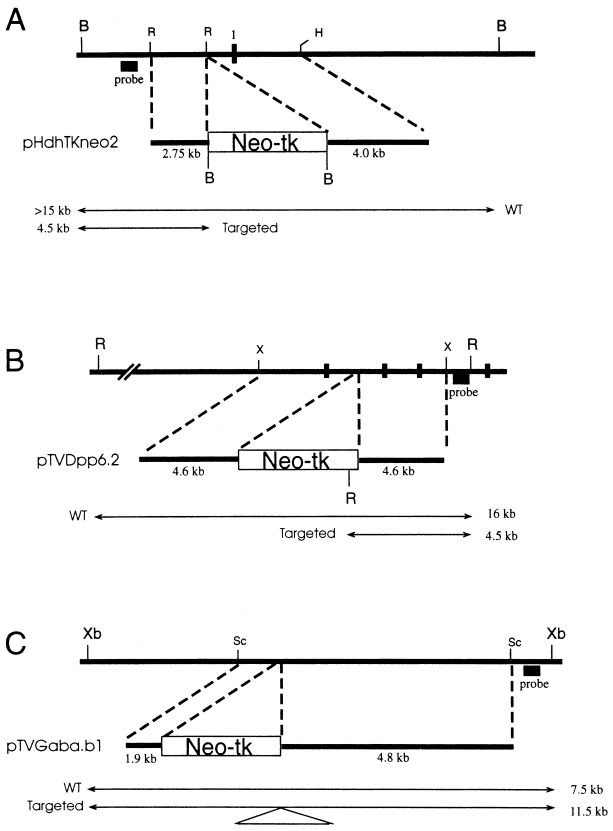

Figure 1 Targeting vectors. (*A*) *Hdh* targeting vector. Transcriptional orientation of the gene is to the right. Note position of exon 1 (1). (*B*) *Dpp6* targeting vector. (*C*) *Gabrb1* targeting vector. In each panel, the genomic locus is shown at the top as a horizontal thick line. Positions of exons are indicated by vertical broken bars. Probes used to detect targeting events are indicated, and the sizes of endogenous (WT) and targeted restriction fragments are shown next to arrows spanning the endpoints. The names of targeting vectors are shown, with the location of the HSV-*tk* (tk)/neomycin resistance (neo) cassette indicated in the large rectangular boxes. (B) *Bam*HI; (R) *Eco*RI; (H) *Hin*dIII; (X or Xb) *Xba* I; (Sc) *Sac*I.

Despite carrying *tk* genes, which are known to disrupt spermatogenesis (Wilkie et al. 1991), at least one clone from each locus yielded germline chimeric males. These clones, or in some cases subclones derived from them, were used for subsequent induction of deletions.

Induction of Deletions

At the *Hdh* locus, two independently targeted germline competent clones were used to induce deletions by subjecting cultures to 400 Gy of gamma radiation from a ^{137}Cs source (see Methods). Both contained the targeted integration on the C57BL/6J allele (B6). Of the ~ 800,000 cells surviving the radiation, ~ 550 survived selection in FIAU, indicating that ~ 1 in 1455 cells had lost expression of the *tk* gene. Three hundred eighty-four FIAU-resistant ($FIAU^R$) colonies were picked and tested for G418 sensitivity, and 96 were screened by PCR (Polymerase Chain Reaction) for presence or ab-

sence of the *tk* gene. Only three G418^R clones were found, indicating that these clones may not have had true deletions, but underwent inactivation of *tk* by epigenetic silencing or mutation. Similarly, 1 clone was *tk* positive by PCR. Overall, the results indicate that the majority of clones were missing the *tk* and neo genes, presumably by radiation-induced deletion, mitotic recombination, or whole chromosome loss. The frequency of *tk* loss (~ 1/1400) was much higher than that (~ 1/20,000) observed at the *D17Aus9* locus (You et al. 1997a).

DNA from these clones then was amplified with primers corresponding to microsatellites polymorphic between the 129 and B6 parental chromosomes. For the initial screen, three markers were used, one just proximal to *Hdh* (*D5Mit148*) and two (*D5Mit1* and *25*) that reside at distances proximal and distal to *Hdh*. The purpose was to eliminate clones that had either: 1) very small deletions (no B6 alleles deleted); 2) large deletions or whole chromosome loss (two or three markers missing); or possible mitotic recombination (retention of the B6 allele of *D5Mit1* but not the distal B6 alleles). A subset of 36 clones appearing to have large interstitial deletions was analyzed with additional markers (Fig. 2 and Table 1; see below).

Induction of deletions at *Dpp6* was conducted in a

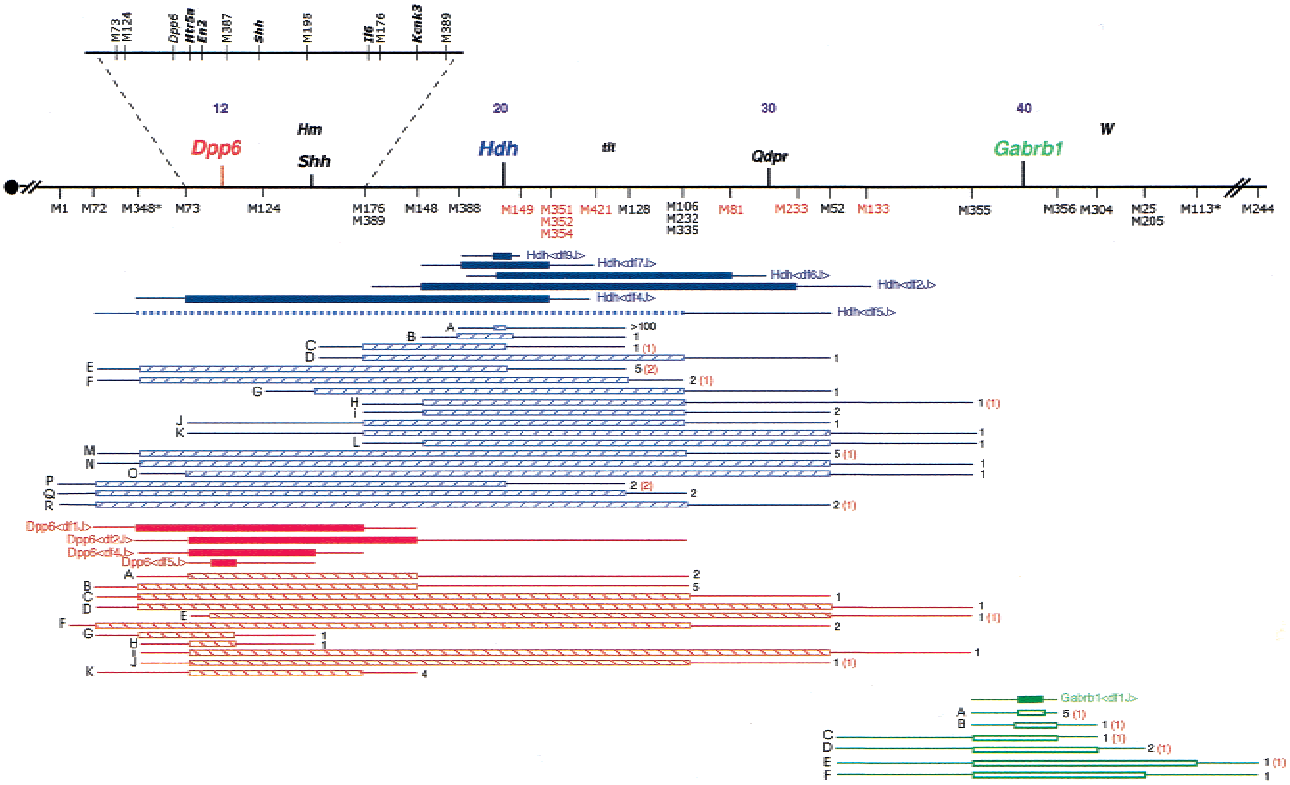

Figure 2 Deletion complexes on chromosome 5. The proximal region of chromosome 5 is depicted as a horizontal line, with the centromere (circle) on the left. Map positions (in centimorgans) as reported in the MGD are indicated, along with the approximate locations of certain landmark loci, such as hammertoe (*Hm*), *Qdpr*, and *Kit*, also known as dominant white spotting (*W*). *Shh* is sonic hedgehog homolog, within which a simple sequence repeat was used to type deletions (see Methods). Microsatellite loci, indicated under the map, have been abbreviated by exchanging the prefix "M" for "D5Mit." The map positions are based on three sources: MGD values, deletion mapping, and RH mapping. As discussed in the text, analysis of deletion breakpoints revealed two disagreements in microsatellite order with MGD; these markers are indicated with asterisks, and in both cases, the MGD order juxtaposes these two markers with the adjacent, proximal microsatellites on this map. A region surrounding *Dpp6* is expanded to integrate data obtained by high resolution RH mapping, as described in the text. Deletions are indicated as horizontal rectangles, either solid, striped, or unfilled, and are color coded with the locus at which they were induced (red, *Dpp6*; blue, *Hdh*; green, *Gabrb1*). The amount of DNA known to be absent in each deletion is spanned by the rectangles. The thin lines extending from the ends of the rectangles indicate the regions in which the deletion breakpoints reside. Those deletions that have been converted into stocks of mice are represented by solid rectangles, and associated allele names are given (the bracketed text corresponds to superscripting). Deletions existing only in ES cells are represented by the striped or unfilled rectangles. In this latter case, the number of independent ES cell lines containing a particular class of deletion (currently indistinguishable with the markers used in this study) is indicated on the right. In some cases, red numbers in parentheses next to these indicate the number of ES cell lines in this deletion class that failed to produce germline chimeras. An ES cell clone containing the *Hdh^{df5J}* deletion, indicated by a dashed line, generated a germline chimera that only transmitted the nondeleted chromosome to its offspring. The relative positions of *D5Mit421*, *tlt* (tilted), and *D5Mit128* are taken from Ying et al. (Ying et al. 1999). Microsatellite markers that are polymorphic between 129 and B6 are in black, whereas those that are not are in red. The following markers had a 129 allele size smaller than B6: *D5Mit1*, *25*, *52*, *72*, *73*, *106*, *124*, *148*, *176*, *232*, *335*, *348*, *356*, *388*,and *Dpp6Rep3*. The remaining SSRs had larger 129 alleles.

Table 1. ES Cell Deletion Lines

DFP	Class	Clone	Germ?	Est. Del. Size	
				Max	Min
Hdh	A	Many			
	B	1-10H/2-2C		6	2
	C	16C/1-B5	Prob. No	8	2
	D	110H/2-8C		12	8
	E	16C/2-1H	No	16	12
		16C/2-7H	No		
		16C/2-4C			
		16C/2-3A			
		16C/2-8D			
	F	16C/2-7F	No	18	16
		16C/2-10A			
	G	16C/2-2A		15	10
	H	16C/2-1D	Prob. No	18	8
	I	16C/2-2B		10	8
		16C/2-1G			
	J	110H/2-11H		17	8
	K	110H/2-5H		25	10
	L	16C/2-9B		18	10
	M	16C/2-1E	No	20	18
		16C/2-1F			
		16C/2-4D			
		16C/2-4G			
		16C/2-8B			
	N	16C/2-4H		28	20
	O	16C/2-8H		28	17
	P	16C/1-D6	No	19	11
		1.10H/2-4B	No		
	Q	16C/2-9D		21	16
		110H/1-6C			
	R	110H/1-4F		23	17
		16C/1-G1	No		
	mice	Hdh<df9J>	Yes	~1	<1
		Hdh<df7J>	Yes	6	2
		Hdh<df6J>	Yes	12	8
		Hdh<df2J>	Yes	14	11
		Hdh<df4J>	Yes	16	9
		Hdh<df5J>	Yes*	20	18
Dpp6	A	2-9d.4/1E		18	7
		2-9d.4/2H			
	B	2-9d.21/8F		18	10
		2-9d.4/2D			
		2-9d.4/4E			
		2-9d.20/5A			
		2-9d.20/6D			
	C	2-9d.4/4F		20	18
	D	2-9d.4/3F		28	20
	E	2-9d.20/6F	No	25	16
	F	2-9d.4/1F		23	18
		2-9d.20/6E			
	G	2-9d.21/8H		8	4
	H	2-9d.21/9F		8	1
	I	2-9d.9/10E		28	17
	J	2-9d.9/10C	No	20	15
	K	2-9d.9/7G		10	7
		2-9d.20/12C			
		2-9d.20/12D			
		2-9d.4/12H			
	mice	Dpp6<df1J>	Yes	10	10
		Dpp6<df2J>	Yes	18	7
		Dpp6<df4J>	Yes	10	5
		Dpp6<df5J>	Yes	5	<1
Gabrb1	A	C136		5	1
		G4			
		14A.C7	No		
		21.B2			
		21.D9			
	B	20.C8	No	5	1
	C	14A.H9		13	5
	D	21.A12		17	5
		2-6F.A1	No		
	E	H4	No	44	6
	F	2-6F.D1		44	9
	mice	Gabrb1<df1J>	Yes	5	<1

similar manner, with one exception. Following the demonstration that one targeted clone (B6 allele) retained germline competence, it was found that this culture contained a high background of FIAU^R cells. Therefore, several subclones were derived that retained essentially complete FIAU sensitivity, and cultures of six of these subclones were irradiated to induce deletions. FIAU^R clones were isolated at a frequency of ~ 1/16,400. Approximately half were G418^S, virtually all of which were shown to have deletions at the molecular level. Thus, the induced deletion rate at *Dpp6* was ~ 1/33,000. As with *Hdh*, a subset of the deletions that appeared to be extremely large, and might actually represent whole chromosome loss or mitotic recombination, were omitted from subsequent analysis of the remainder with a panel of microsatellite markers.

Recovery of deletions at the *Gabrb1* locus was less efficient. Only ~ 2–5% of FIAU-resistant clones were, in fact, missing the *tk* gene after irradiation (presumably the rest underwent epigenetic silencing of *tk* expression), and many of these had undergone either extremely large deletions or mitotic recombination (showing LOH [Loss of Heterozygosity] of *D5Mit1*, *D5Mit244*, or both). Nevertheless, 13 interstitial deletions were obtained (of which 12 were analyzed in detail), falling into several classes (see below).

Molecular Mapping of Deletion Breakpoints and Interdigitation of Deletion Complexes

The deficiencies at each of the three DFPs had a range of sizes and breakpoints. As shown in Figure 2, there was a large degree of overlap between the *Hdh* and *Dpp6* deletions, forming an indigitated collection. Some of the deletions were extremely large, extending ~ 20 cM or more in length (using map positions currently reported in the MGD [Mouse Genome Database]; the minimum and maximum deletion sizes are listed in Table 1). Although the breakpoints of several independent deletions are currently indistinguishable, this is attributable to the limited number of polymorphic microsatellites available for the parental (129 and B6) genotype of the ES cells. Higher resolution analysis of some deletions was attainable by crossing mice derived from deletion-bearing ES cells (see next section) to *Mus castaneous* and analyzing DNA from the resulting F_1 interspecific hybrids.

(DFP) Deletion focal point. (Class) corresponds to the codes in Figure 2. (Clone) lab codes for all deletion lines in a particular class. (Germ) refers to whether the indicated clones generated germline chimeras. The maximum and minimum deletion sizes in centimorgans were determined using current MGD values.
*The cell line with this deletion underwent germline transmission, but the deletion chromosome itself was not transmissable.

Interestingly, there was no evidence for overlap of deletions originating from the *Hdh* and *Gabrb1* loci, although several breakpoints from both deletion complexes lie between the *Qdpr* and *Gabrb1* loci, within the *D5Mit52* to *D5Mit355* interval. Although the apparent lack of overlap may be a consequence of the dearth of polymorphic markers in the region, it is possible that there is a locus or loci in this interval that cannot exist in the haploid state in ES cells. Because the *Hdh* deletions occurred on the B6 chromosome, and the *Gabrb1* deletions occurred on 129, it is unlikely that such a haploinsufficiency is caused by parental chromosome-specific imprinting, although the possibility that two loci are present that are oppositely imprinted remains.

Creation of Mice Bearing Deletions

Several deletion-bearing ES cell clones were injected into B6 blastocysts to generate chimeric animals. Chimeras then were mated to B6 to check for germline transmission. Although all agouti animals from such a mating must be ES-cell derived, some black animals were also ES cell-derived, because the v6.4 cells are heterozygous for a B6 allele at the agouti locus. In most cases, a deletion clone was injected on only one or two occasions, so the failure of a clone to yield germline chimeras may reflect technical issues rather than true ability of an ES cell clone to colonize the germline.

Of 17 injected TK- clones from the *Hdh* locus, eight were shown capable of making germline chimeras. Two of these were not true deletions; one was a mitotic recombinant, and the other had LOH of several markers apparently caused by a double crossover or event of similar consequence. Another (Hdh^{df5J}; dashed blue line in Fig. 2) was a large deletion that yielded germline chimeras; however, the agouti progeny produced by these chimeras exclusively inherited the nondeleted (129) chromosome. Five clones bearing deletions of various sizes ultimately were established as lines of mice (solid blue lines in Fig. 2). Cell lines bearing deletions that did not produce germline chimeras are indicated by red numbers in parentheses next to the corresponding deletion class (depicted as patterned lines in Fig. 2). Seven such clones contained deletions extending proximally past *D5Mit72* and/or *D5Mit348* loci that were not deleted in clones showing germline transmission. This suggests that the primary reason for failure of germline transmission might be related to the deletion size or hemizygosity of particular loci, rather than problems caused by the irradiation and selection.

Similar results were obtained with deletions induced at the *Dpp6* locus. Six deletion lines were injected into blastocysts, and four ($Dpp6^{df1J,\ 2J,\ 4J}$ and ^{5J}) produced chimeras that transmitted the deletion chromosomes to progeny (Fig. 2). The two cell lines that failed to produce germline chimeras contained extremely large deletions that extended past *D5Mit232*. Once again, we suspect that the failure of these two lines is related to the large size of the deletions.

A more drastic example of deletion size compromising the ability of ES cells to colonize the germline was experienced with deletions induced at the *Gabrb1* locus. Only one of six blastocysts-injected deletion clones yielded germline chimeras, and this particular line contained a small deletion that did not remove any flanking microsatellite markers. Four of the remaining five deletions removed one or more markers, and these either failed to produce chimeric mice or the chimeras derived from them had poor contribution from the injected ES cells, judging from the low proportion of agouti fur in the coat (the C57BL/6J host blastocysts produce a black coat). We conclude that there is a haploinsufficient locus or loci near the *Gabrb1* locus that, when present in only a single copy, is incompatible with development of most tissues or cell types. At present, we cannot determine whether this locus (or loci) is located proximal, distal, or on both sides of *Gabrb1*. Unfortunately, this would appear to preclude the generation of large deletions in this immediate region.

Deletions as Mapping Reagents

An ancillary benefit of the deletions is that they provide an excellent tool for determining the relative orders of polymorphic loci along chromosomes. The map locations of most microsatellites remains exclusively deduced from the relatively small (48 progeny) F_2 mapping cross performed by the Whitehead Institute Genome Center. Higher resolution crosses performed by others, including the EUCIB (European Collaborative Interspecific Backcross; www.hgmp.mrc.ac.uk/MBx/MBxHomepage.html) usually include only a subset of these markers and "anchor" loci. In the course of typing the deletions for the array of markers illustrated in Figure 2, we uncovered two inconsistencies in marker order as represented in MGD as of May 2000. *D5Mit72* must be proximal rather than distal to *D5Mit348*, because 15 *Hdh* deletions and nine *Dpp6* deletions removed *D5Mit348* but not *D5Mit72*. Analysis of *Gabrb1* deletions indicated that *D5Mit113* (42.0 cM; MGD) is distal to *D5Mit25* and *D5Mit205* (45.0 cM; MGD); one ("E" in Fig. 2) deletion was found that removed the latter two but not the former. However, it is possible that this deletion is complex or not continuous, as has been observed with classically induced deletions (Sharan et al. 1991; Johnson et al. 1995).

The collection of deletion breakpoints also was able to separate markers that were previously nonrecombinant in mapping crosses (and reflected in MGD). One such nonrecombinant group was *D5Mit148*,*176*, *388*, and *389*. Deletion analysis enabled these to be subdivided into three intervals (Fig. 2). It also was possible to separate one microsatellite marker from each of

two other clusters that contained three inseparable loci, *D5Mit83/304/356* and *D5Mit25/153/205* (Fig. 2).

Complementation Analysis Indicates Hammertoe (Hm) Is Not a Null Mutation

Hm is a semidominant mutation located proximal to *Hdh* and apparently distal to *Dpp6*. Although it has not been mapped in the same cross as *Dpp6*, *Hm* was shown to be extremely close but just proximal to hemimelic extra toes (*Hx*), recombining once in 3664 offspring (~ 0.03 cM; Sweet 1982). *Hx* was shown to be distal to *En2* (Robert et al. 1994), which is, in turn, distal to *Dpp6* as reported in The Jackson Laboratory's BSS interspecific backcross and two independent crosses (Wada et al. 1993; Montgomery et al. 1994), resulting in MGD consensus locations of 12 and 16 cM for *Dpp6* and *Hm*, respectively. Mice heterozygous for *Hm* retain skin between their digits, giving the appearance of webbed paws. Homozygotes display a more severe phenotype, in which the digits are severely curled and essentially attached (although not polysyndactylous). The deficiency Hdh^{df4J} probably removes the *Hm* locus because it extends proximal to *Dpp6* and distal to *Hdh*. However, Hdh^{df4J} heterozygotes do not possess webbed paws, indicating that *Hm* is not a loss-of-function mutation. Furthermore, Hdh^{df4J}/*Hm* animals are phenotypically identical to *Hm*/ +, not having the more severe phenotype characteristic of *Hm* homozygotes (not shown). These observations indicate that the hammertoe mutation is a gain-of-function allele. We caution, however, that this conclusion relies on the assumption that *Hm* maps distal to *Dpp6*.

DISCUSSION

The work described here illustrates the power of the radiation-induced deletion technique for rapidly saturating large chromosome regions with deficiencies of all sizes. Only a single targeted ES cell clone is needed to yield an unlimited number of different deletions in a single experiment, with staggered breakpoints in both directions. Importantly, our data suggest that the exposure of the cells to radiation, which may cause second site mutations and other biological responses, has little deleterious consequence on the germline-colonizing potential of ES cells. Rather, it appears that haploidy of particular genomic regions is the primary determinant of whether a deletion-bearing ES cell can create germline chimeric mice. This is a biological issue that appears to be independent of the technology itself. Similar observations were made in the cases of large deletions created by Cre-loxP recombination (Liu et al. 1998).

There are probably three factors that influence whether a deletion will be lethal or prevent the formation of chimeras. One is the overall size, such that hemizygosity of increasing numbers of genes incrementally decreases fitness. A second factor may have to do with the existence of a strictly haploinsufficient locus, which when deleted, abolishes pluripotentiality of ES cells. In this situation, deletions emanating from a particular DFP would be inviable once they extend past a given point. This might be the case with the *Gabrb1* deletions. Notably, we have observed a high rate of peri- and postnatal lethality (60%) of mice heterozygous for the W^{19H} deletion, which covers the *D5Mit83-D5Mit112* interval just distal to *Gabrb1* (King et al. 1997; G. Leach and M. Bucan, unpubl.). A final possibility is that there exists an imprinted locus, near the DFP, that is active only on the targeted chromosome (in the *Gabrb1* case, 129). Because ES cells maintain their genomic imprinting, a deletion of the active allele essentially would create nullizygosity for expression of the imprinted gene; if that gene were required for either germ cell development or early embryogenesis, this would abolish the ability of the ES cell to make germline chimeras. From a technical viewpoint, if one desired to make and propagate mice bearing deletions in a region in which this was the case, then the *tk*-neo cassette should be targeted to the chromosome bearing the silenced allele, exploiting the preference of an exogenous vector to undergo homologous recombination with an isogenic target (teRiele et al. 1992).

Interestingly, the experiments provided evidence for the existence of a gene or genes that are haploinsufficient for growth of ES cells near the *Gabrb1* locus. Evidence for haploinsufficient loci on chromosome 9 in ES cells also was reported by Thomas et al., who created a radiation-induced deletion complex at the *Ncam* locus (Thomas et al. 1998), and Zheng et al., who induced deletions on chromosome 11 with a targeted Cre-loxP strategy (Zheng et al. 2000).

The utility of deletion complexes, rather than individual deletions, lies in downstream applications for dissecting genome function. In mice, deletion complexes created by whole animal irradiation experiments have been generated around several visibly scorable loci, including albino (Tyr^{c}), brown ($Tyrp1^{b}$), pink-eyed dilution (*p*), short ear ($Bmp5^{se}$), nonagouti (*a*), dilute ($Myo5a^{d}$), and piebald ($Ednrb^{s}$). A systematic characterization of functional units along these chromosomal regions has been performed with the brown and albino deletions in particular to identify genes important in development (Russell et al. 1982; Rinchik and Russell 1990; Holdener-Kenny et al. 1992; Rinchik et al. 1994). In these studies, different deletions from the same deletion complex were crossed to one another or rendered homozygous, and the phenotypes associated with nullizygosity of various regions were delineated and, in one case, ultimately cloned (Schumacher et al. 1996). However, a drawback to this approach is that early acting deletions that are very close to the DFP will mask functions encoded in more dis-

tant locations. The availability of adjacent deletion complexes obviates this problem, enabling the creation of complex heterozygotes that are nullizygous for intervals in between the DFPs (You et al. 1997b). The deletion complexes described here enable such an approach for the overlapping *Hdh* and *Dpp6* deletions.

To increase the value of deletion complexes described in this article, we integrated the deletion map with marker-dense RH (Radiation Hybrid) and genetic maps that, for this 40-cM chromosomal region, include > 90 genes and 200 SSLP (Simple Sequence Length Polymorphism) markers (Tarantino et al. 2000). By placing a set of common SSLP markers on all three maps, it is now possible to provisionally determine or predict a set of genes missing in each overlapping deletion. For example, the integrated map allows us to predict that the genes *Dpp6*, *Htr5a*, *En2*, *Shh*, *Il6*, and *Kcnk3* are deleted in $Dpp6^{df2J}$ (*D5Mit73* to *D5Mit389* interval). Current efforts to place novel expressed sequence tags on the RH map and to eventually sequence the mouse genome will allow more accurate prediction of genes deleted in the individual lines, and therefore facilitate the identification of candidate genes for abnormal phenotypes associated with these deletions.

A principal motivation for establishing these deletion complexes was to conduct an ENU saturation mutagenesis screen of the *Rw* inversion region of chromosome 5 (Schimenti and Bucan 1998). The *Rw* inversion spans a 30-cM region between the *Dpp6* and *Kit* (*W*) loci (see Fig. 2). The two generation screen for detection of ENU-induced mutations is being performed by crossing animals carrying ENU-exposed chromosomes in *trans* to the *Rw* balancer to deletion-bearing mice and phenotyping (for visible anomalies) only those animals that contain the deletion in *trans* to the mutagenized chromosome. To span the *Rw* region as efficiently as possible, a set of deletions representing a minimum tiling path is being used. For example, the two deletions $Dpp6^{df1J}$ and Hdh^{df2J} together span > 22 cM. The value of a nested deletion set is that it serves as a powerful and rapid resource for mapping newly induced recessive mutations. The random nature of the breakpoints on both ends of each deletion confers bidirectional mapping utility.

The ability to create deletion complexes also should prove valuable in modeling human contiguous gene syndromes such as Cri-du-chat, Williams-Beuren, and Jacobson. This generation of a mouse strain bearing a deletion corresponding to the DiGeorge syndrome region demonstrated this point (Lindsay et al. 1999). The deletions described here will be relevant for modeling and mapping loci involved in WHS (Wolf-Hirshhorn syndrome), the critical region of which is located within a megabase of *Hdh* (Wright et al. 1997). The large collection of *Dpp6* and *Hdh* deletions already existing as mouse strains, plus those remaining cryopreserved in ES cells, potentially can be used to dissect regions corresponding subphenotypes of this syndrome that may be manifested in mice. Indeed, several of the *Hdh* deletions have presented defects reminiscent of WHS (D. Naf and J.C. Schimenti, unpubl.).

METHODS

Targeting Constructs

Hdh

The plasmid pHdh-2, containing the downstream 4-kb arm of the *Hdh* targeting vector (Fig. 1) as an *Eco*RI/*Hin*dIII insert, was linearized with *Not*I, Klenow filled, *Bam*HI digested (cleaving at a site within the polylinker adjacent to the *Eco*RI site), and ligated to the 2.75-kb upstream arm excised from plasmid pHdh-1 (which contained the arm as an *Eco*RI fragment) by linearizing with *Cla*I, Klenow filling, and cleaving with *Bam*HI. This intermediate plasmid was linearized with *Bam*HI (cleaving at the junction between the two arms) and ligated to a 4-kb *Bam*HI *tk*-neo cassette fragment excised from pBSSKΔBam (You et al. 1997a).

Dpp6

A 9.2-kb *Xba*I genomic fragment containing three exons of *Dpp6*, isolated from cosmid cAB1 cloned from a *Rw*/+ library (Hough et al. 1998) was subcloned into the vector pBSSKΔBam (You et al. 1997a) to create pX8–1. A 4.0-kb *Bam*HI fragment containing a neo-*tk* cassette then was subcloned, in both orientations, into an unique *Bam*HI site near the center of the 9.2-kb *Xba*I insert of pX8-1. The resulting targeting vectors were called pTVDpp6.1 and pTVDpp6.2. These vectors were linearized with *Not*I for electroporation into ES cells.

Gabrb1

A 6.7-kb *Sac*I genomic fragment, isolated from bacterial artificial chromosome 388L8 (Lengeling et al. 1999) and derived from the CITB 129/Sv library (Research Genetics, Huntsville, AL), was subcloned into pBSSKΔBam, and the Neo-*tk* cassette subsequently was inserted into a unique *Bam*HI site, resulting in 1.9 kb of homology on one side of the cassette, and 4.8 kb on the other. The resulting targeting vector was called pTVGaba.b1. The vector was linearized with *Not*I for electroporation into ES cells.

ES Cell Culture, Irradiation, and Selection

Detailed protocols for inducing and selecting deletions have been published elsewhere (You et al. 1997b). Briefly, targeted ES cell clones were grown in G418-containing medium on a feeder layer until the time they were trypsinized and irradiated, in suspension, with 400 Gy from a ^{137}Cs source. In general, 2×10^6 irradiated cells were plated onto gelatin-coated, feederless, 150-mm culture dishes, in leukemia inhibitory factor–containing medium without selection. FIAU was added after 72 hours, and this selection was continued for 3 days, with daily medium changes. After selection, the cells were grown until colonies were of a sufficient size to pick into 96-well plates as described (Ramirez-Solis et al. 1993). DNA was prepared either according to that method or by crude lysis overnight at 55 °C in PBND (50 mM KCL, 10 mM Tris, pH 8.3, 2.5 mM $MgCl_2$, 0.1 mg/ml gelatin, 0.45% NP40, 0.45% Tween 20, 50 µg/ml proteinase K) if the samples were to be used

exclusively for PCR. One microliter or less of such a lysate was used for PCR.

Microsatellite Marker Analysis

Most microsatellite PCR products were analyzed on 3–3.5% Metaphor gels (FMC). Because these gels may not detect size differences of 1 or 2 bp, it is possible that some of the markers listed as nonpolymorphic may indeed be so. The strains tested for SSLPs were 129/SvJae (extracted from J1 ES cells) and C57BL/6J, the parental strains of the v6.4 ES cells. Markers that we discovered to be polymorphic between 129/SvJae and C57BL/6J are indicated in Figure 2, and the relative allele sizes are indicated in the legend. Two new polymorphic microsatellites were identified to screen all deletions at *Dpp6*: *Dpp6Rep3* (primers ctattcctagagttcacatggtgg and acagaaatac-cagttcctagaacc) and *Dpp6Rep4* (agacaggcagactccctcaagagg and cctcaagtcctctttctgctttgg). A polymophic microsatellite at the *Shh* locus was amplified with the primers CCTggTCCAACC-gAgTgAgAC and CCACggAgTTCTCTgCggAg.

ACKNOWLEDGMENTS

This work was supported by grants HD35984 to J.C.S. and HD24180 to M.B. We thank Karen Moore for providing data on 129 versus B6 polymorphisms; Marcy MacDonald for *Hdh* clones; and Tim O'Brien and Wayne Frankel for critical reading of the manuscript.

The publication costs of this article were defrayed in part by payment of page charges. This article must therefore be hereby marked "advertisement" in accordance with 18 USC section 1734 solely to indicate this fact.

REFERENCES

Duyao, M.P., Auerbach, A.B., Ryan, A., Persichetti, F., Barnes, G.T., McNeil, S.M., Ge, P., Vonsattel, J.P., Gusella, J.F., Joyner, A.L., et al. 1995. Inactivation of the mouse Huntington's disease gene homolog *Hdh*. *Science* **269:** 407–410.

Green, P. 1997. Against a whole-genome shotgun. *Genome Res*. **7:** 410–417.

Holdener-Kenny, B., Sharan, S.K., and Magnuson, T. 1992. Mouse albino-deletions: From genetics to genes in development. *Bioessays* **14:** 831–839.

Hough, R.B., Lengeling, A., Bedian, V., Lo, C., and Bucan, M. 1998. Rump white inversion in the mouse disrupts dipeptidyl aminopeptidase-like protein 6 and causes dysregulation of *Kit* expression. *Proc. Natl. Acad. Sci. USA* **95:** 13800–13805.

Johnson, D.K., Stubbs, L.J., Culiat, C.T., Montgomery, C.S., Russell, L.B., and Rinchik, E.M. 1995. Molecular analysis of 36 mutations at the mouse pink-eyed dilution (*p*) locus. *Genetics* **141:** 1563–1571.

King, D.P., Vitaterna, M.H., Chang, A.M., Dove, W.F., Pinto, L.H., Turek, F.W., and Takahashi, J.S. 1997. The mouse Clock mutation behaves as an antimorph and maps within the W19H deletion, distal of Kit. *Genetics* **146:** 1049–1060.

Lengeling, A., Wiltshire, T., Otmani, C., and Bucan, M. 1999. A sequence-ready BAC contig of the GABAA receptor gene cluster *Gabrg1–Gabra2-Gabrb1* on mouse chromosome 5. *Genome Res*. **9:** 732–738.

Lindsay, E.A., Botta, A., Jurecic, V., Carattini-Rivera, S., Cheah, Y.C., Rosenblatt, H.M., Bradley, A., and Baldini, A. 1999. Congenital heart disease in mice deficient for the DiGeorge syndrome region. *Nature* **401:** 379–383.

Liu, P., Zhang, H., McLellan, A., Vogel, H., and Bradley, A. 1998. Embryonic lethality and tumorigenesis caused by segmental aneuploidy on mouse chromosome 11. *Genetics* **150:** 1155–1168.

Montgomery, J., Guarnieri, M., Tartaglia, K., and Flaherty, L. 1994. High-resolution genetic map and YAC contig around the mouse neurological locus reeler. *Mamm. Genome* **5:** 756–761.

Ramirez-Solis, R., Davis, A., and Bradley, A. 1993. Gene targeting in embryonic stem cells. *Methods Enzymol*. **225:** 855–877.

Rinchik, E., and Russell, L. 1990. Germ-line deletion mutations in the mouse: Tools for intensive functional and physical mapping of regions of the mammalian genome. *Genome Anal*. **1:** 121–158.

Rinchik, E., Bell, J., Hunsicker, P., Friedman, J., Jackson, I., and Russell, L. 1994. Molecular genetics of the brown (*b*)-locus region of mouse chromosome 4: Origin and molecular mapping of radiation and chemical induced lethal brown deletions. *Genetics* **137:** 845–854.

Robert, B., Montagutelli, X., Houzelstein, D., Ferland, L., Cohen, A., Buckingham, M., and Guenet, J.L. 1994. *Msx1* is close but not allelic to either *Hm* or *Hx* on mouse chromosome 5. *Mamm. Genome* **5:** 446–449.

Russell, L., Montgomery, C., and Raymer, G. 1982. Analysis of the albino-locus region of the mouse. IV. Characterization of 34 deficiencies. *Genetics* **100:** 427–453.

Schimenti, J., and Bucan, M. 1998. Functional genomics in the mouse: Phenotype-based mutagenesis screens. *Genome Res*. **8:** 698–710.

Schumacher, A., Faust, C., and Magnuson, T. 1996. Positional cloning of a global regulator of anterior-posterior patterning. *Nature* **383:** 250–253.

Sharan, S.K., Holdener Kenny, B., Ruppert, S., Schedl, A., Kelsey, G., Rinchik, E.M., and Magnuson, T. 1991. The albino-deletion complex of the mouse: Molecular mapping of deletion breakpoints that define regions necessary for development of the embryonic and extraembryonic ectoderm. *Genetics* **129:** 825–832.

Sweet, H. 1982. *Hm* and *Hx* are not alleles. *Mouse News Lett*. **66:** 66.

Tarantino, L., Feiner, L., Alavizadeh, A., Wiltshire, T., Hurle, B., Ornitz, D., Webber, A., Raper, J., Rowe, L., Lengeling, A., et al. 2000. A high-resolution radiation hybrid map of the proximal portion of mouse chromosome 5. *Genomics* **66:** 65–75.

teRiele, H., Maandag, E., and Berns, A. 1992. Highly efficient gene targeting in embryonic stem cells through homologous recombination with isogenic DNA constructs. *Proc. Nat. Acad. Sci. USA* **89:** 5128–5132.

Thomas, J.W., LaMantia, C., and Magnuson, T. 1998. X-ray-induced mutations in mouse embryonic stem cells. *Proc. Natl. Acad. Sci. USA* **95:** 1114–1119.

Wada, K., Zimmerman, K.L., Adamson, M.C., Yokotani, N., Wenthold, R.J., and Kozak, C.A. 1993. Genetic mapping of the mouse gene encoding dipeptidyl aminopeptidase-like proteins. *Mamm. Genome* **4:** 234–237.

Weber, J.L., and Myers, E.W. 1997. Human whole-genome shotgun sequencing. *Genome Res*. **7:** 401–409.

Wilkie, T.E., Braun, R.E., Ehrman, W., Palmiter, R., and Hammer, R. 1991. Germ-line intrachromosomal recombination restores fertility in transgenic MyK-103 male mice. *Genes Dev*. **5:** 38–48.

Wright, T.J., Ricke, D.O., Denison, K., Abmayr, S., Cotter, P.D., Hirschhorn, K., Keinanen, M., McDonald-McGinn, D., Somer, M., Spinner, N., et al. 1997. A transcript map of the newly defined 165 kb Wolf-Hirschhorn syndrome critical region. *Hum. Mol. Genet*. **6:** 317–324.

Ying, H.C., Hurle, B., Wang, Y., Bohne, B.A., Wuerffel, M.K., and Ornitz, D.M. 1999. High-resolution mapping of *tlt*, a mouse mutant lacking otoconia. *Mamm. Genome* **10:** 544–548.

You, Y., Bergstrom, R., Klemm, M., Lederman, B., Nelson, H., Ticknor, C., Jaenisch, R., and Schimenti, J. 1997a. Chromosomal deletion complexes in mice by radiation of embryonic stem cells. *Nat. Genet*. **15:** 285–288.

You, Y., Browning, V.L., and Schimenti, J.C. 1997b. Generation of radiation-induced deletion complexes in the mouse genome using embryonic stem cells. *Methods* **13:** 409–421.

You, Y., Bersgtram, R., Klemm, M., Nelson, H., Jaenisch, R., and Schimenti, J. 1998. Utility of C57BL/6J × 129/SvJae embryonic stem cells for generating chromosomal deletions: Tolerance to gamma radiation and microsatellite polymorphism. *Mamm. Genome* **9:** 232–234.

Zheng, B., Sage, M., Sheppeard, E.A., Jurecic, V., and Bradley, A. 2000. Engineering mouse chromosomes with Cre-loxP: Range, efficiency, and somatic applications. *Mol. Cell. Biol*. **20:** 648–655.

Received March 3, 2000; accepted in revised form May 10, 2000.